ISSN 1062-8738, Bulletin of the Russian Academy of Sciences: Physics, 2024, Vol. 88, No. 6, pp. 991–995. © Pleiades Publishing, Ltd., 2024.

Estimating Detection Depth of Hydrodynamic Structures in Water through Above-Surface Optical Information Analysis

N. A. Lipinskaya[a], * (ORCID: 0000-0002-3177-4426) **and P. A. Salyuk**[a], ** (ORCID: 0000-0002-3224-710X)

[a] *Il'ichev Pacific Oceanological Institute, Far Eastern Branch, Russian Academy of Sciences, Vladivostok, 690041 Russia*

**e-mail: lipinskaya.na@poi.dvo.ru*

***e-mail: psalyuk@poi.dvo.ru*

Received December 15, 2023; revised January 29, 2024; accepted February 26, 2024

Abstract—We describe a method for estimating detection depth of underwater hydrodynamic structures in above-water optical data. In situ and remote sensing data, as well as numerical modeling of the formation of upward radiation from the water surface are used for the design. The results of this study improve the interpretation of spectral data obtained from remote sensing of water color, which is associated with vertical variations in the content of optically active substances. Additionally, the method allows for determining the thickness of the surface layer within which some hydrodynamic phenomena can be remotely detected in the visible spectral range.

Keywords: remote sensing, optics, numerical modeling, hydrodynamic structures

DOI: 10.1134/S1062873824706962

INTRODUCTION

This work is based on measurements and calculations obtained for marine waters, but the results can be adapted to any natural or artificial water bodies and reservoirs. Hydrodynamic phenomena in the ocean have a significant impact on the spatial and temporal redistribution of optically active substances (OAS) that scatter or absorb light in the water [1–3]. In natural aquatic environments, the main OAS are phytoplankton cells, colored dissolved organic matter (CDOM), organic and mineral suspended particles, and gas bubbles [4]. The redistribution of the content of OAS affects the vertical and horizontal distribution of inherent optical properties of seawater, which, in turn, affects the spectral composition of the upward radiation from the sea surface [5, 6].

Modern development of numerical models that consider the system "atmosphere–sea surface–sea column" [7] allows us to study the formation of spectral remote sensing reflectance of seawater (*Rrs*) depending on the variability of vertical profiles of the content of OAS in seawater [8]. The application of numerical modeling of the spectral color of the sea expands the possibilities of studying hydrodynamic phenomena in the ocean. For example, estimation of the depth at which the position of the chlorophyll-a (chl-a) concentration maximum layer significantly affects the spectral remote sensing reflectance of the sea can be used to separate the influence of biological and direct hydrodynamic factors on the variations of satellite estimates of chl-a concentration [9] or to estimate the depth at which the contrasts of submesoscale eddies are formed in satellite sea color data [10].

The purpose of this work is to develop a universal method for estimating the thickness of the sea surface layer, where the upwelling radiation of the sea is formed with the possibility of identifying the hydrodynamic structure in the sea color remote sensing data (detection depth of hydrodynamic structure—Z_{rs}).

DATA AND METHODS

In this work we used the data set containing data of marine expeditionary studies and archived satellite data with manifestations of hydrodynamic processes:

— in situ measurements in the seawater column: depth profiles of bio-optical and hydrological parameters from SeaBird SBE-19plus and SBE-911 probes (temperature, salinity) with WetLabs, SeaPoint and Chelsea Minitracka II chl-a fluorescence sensors, CDOM fluorescence sensor; measurements of bio-optical and hydrological parameters from the flow-through system on horizontal transects at a depth of 4–5 m, obtained by SeaBird SBE-21 and SBE-45 thermosalinographs (temperature, salinity), and a laser hyperspectral fluorimeter of seawater (chl-a fluorescence and CDOM).

— remote surface data of visible and infrared bands: Measurements of *Rrs* spectra from the shipboard side using an ASD FieldSpec Hand Held hyper-

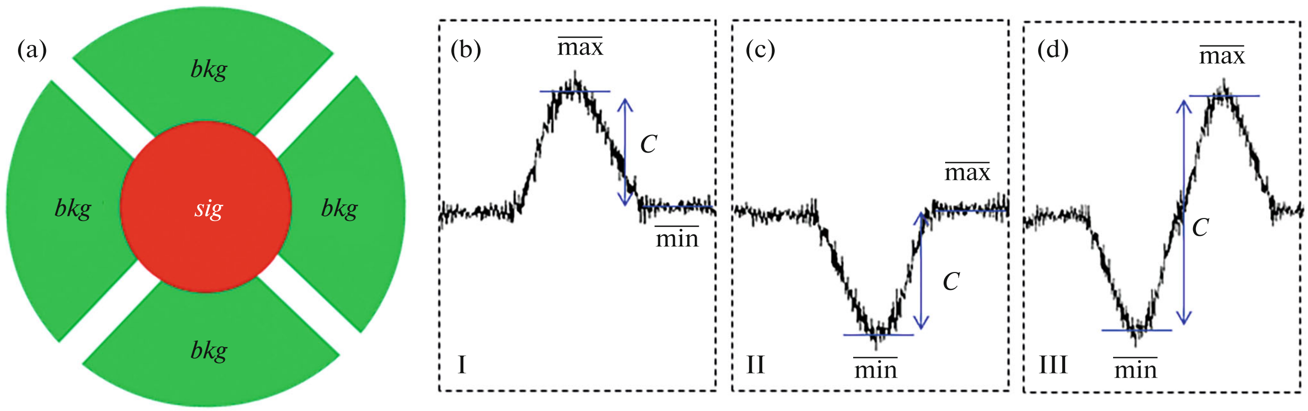

Fig. 1. Scheme of signal and background determination in the area of hydrodynamic process action.

spectral radiometer using techniques from NASA protocols [11]; the second level of average spatial resolution of spectroradiometers MODIS-Aqua/Terra, OLCI-Sentinel-3A/-3B, GOCI/COMS (pixel size 250–2000 m) (sea surface temperature, chl-a concentration estimates using global empirical algorithms of CI and OCx family [12], multichannel *Rrs* measurements).

Additionally, regional tuning of the bio-geo-optical models of the Hydrolight-Ecolight 6.0 package [7] was performed in order to calculate *Rrs* spectra depending on the vertical distribution of the content of the main optically active substances in the water column. In this work, the listed in situ measurement data were used as input parameters and remote sensing data were used as validation data. The parameters of regional settings of bio-geo-optical models were selected so as to minimize the total error between measured and modeled *Rrs* values [9, 10, 13].

RESULTS AND DISCUSSION

The contrast to noise ratio (*CNR*) was used as a characteristic to assess the quality of hydrodynamic structure detection. The contrast is the difference between the remotely measured signal inside the hydrodynamic structure (*sig*) and remotely measured signal outside the hydrodynamic structure (*bkg*) (Fig. 1a). The noise estimation was the standard deviation of the smallest of the signals.

If *sig* > *bkg* (Fig. 1b), then *sig* is the maximum of smoothed data ($\overline{\max}$), and *bkg* is the minimum of smoothed data ($\overline{\min}$). In case *sig* < *bkg* (Fig. 1c), then vice versa. When in the region inside the hydrodynamic structure there is both a local maximum and a local minimum (Fig. 1d), the value of *sig* is equal to $\overline{\max}$, and *bkg* is equal to $\overline{\min}$.

The contrast (*C*) was determined from the difference of the obtained *sig* and *bkg* values. The noise estimation was determined by the value of the mean square deviation of *sig* (σ_{sig}) or *bkg* (σ_{bkg}), depending on which of the signals was smaller. Thus, the *CNR* was determined by the following formula:

$$CNR = \frac{sig - bkg}{noise} = \frac{C}{\min(\sigma_{sig}, \sigma_{sig})}. \quad (1)$$

Similar definitions are widely used in various studies related to the analysis of structures in images [14, 15]. We do not introduce a module to define the contrast, since the sign carries additional information about the type of hydrodynamic structure. The obtained absolute value $|CNR|$ can be interpreted as the maximum possible contrast resulting from the presence of the hydrodynamic structure with respect to the variability of the "background" signal. This value is necessary to assess the possibility of detecting the hydrodynamic structure in the remote sensing data of spectral characteristics of sea color. If $|CNR| > 1$, the contrast can be considered significant and the corresponding structure should be manifested in the remote sensing data. In this case, if a sufficiently large number of adjacent points (pixels) of measurements will have $|CNR| > 0.5$, then such a structure can also be identified by modern methods of structure recognition in the measurement data.

In this work, *CNR* values were calculated for the following remotely detectable characteristics: $Rrs(\lambda)$, band-ratios $BR(\lambda)$, chl-a concentration (*chlor_a*), where

$$BR(\lambda) = \frac{Rrs(\lambda)}{Rrs(555)}, \quad (2)$$

$$\log(chlor_a) = a_0 + \sum_{i=1}^{4} a_i \left(\log\left(\frac{Rrs(\lambda_{blue})}{Rrs(\lambda_{green})} \right) \right), \quad (3)$$

where $Rrs(\lambda_{blue})$ is the maximum of several values of $Rrs(\lambda)$ in the blue spectral region 440–520 nm, $Rrs(\lambda_{green})$ corresponds to the measurement of *Rrs* around 555 nm, and the coefficients a_i are selected for a specific satellite optical radiometer [16].

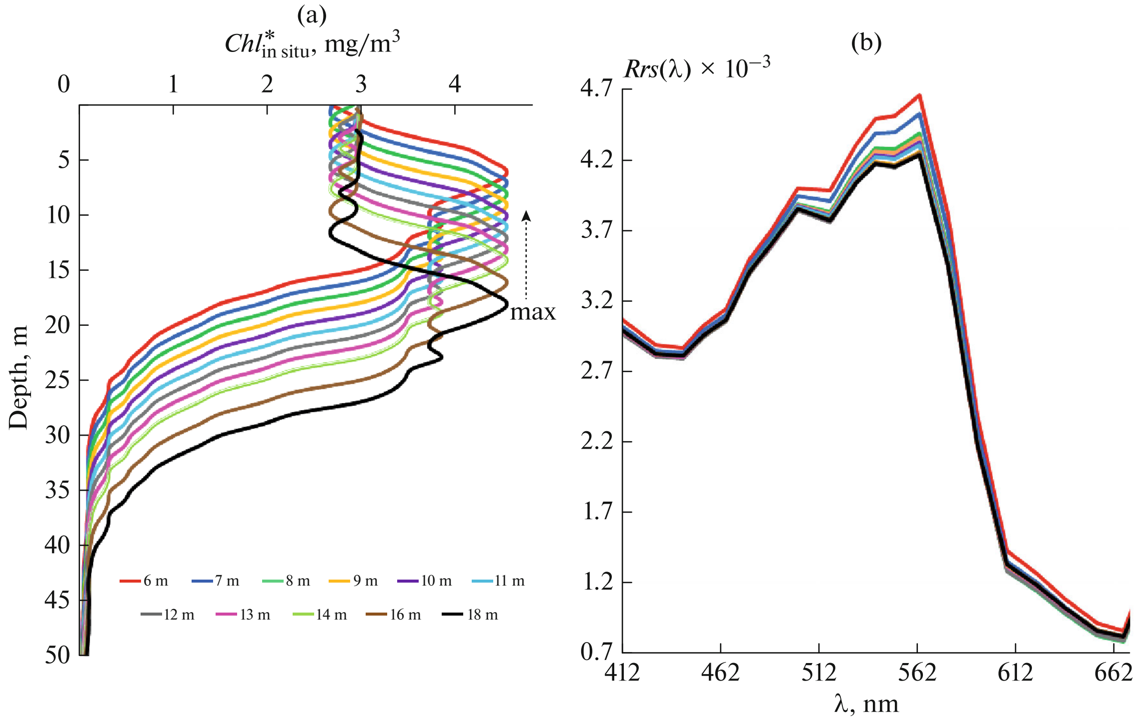

Fig. 2. (a) Simulation of the upward of the vertical profile of the chl-a concentration measured in situ ($Chl_{\text{in situ}}$); (b) results of numerical modeling of the $Rrs(\lambda)$ spectrum as a function of changes in the depth of the chl-a concentration maximum.

To determine the detection depth of hydrodynamic structure Z_{rs}, we used tuned bio-geo-optical models in the Hydrolight-Ecolight 6.0 software, the input of which was fed not measured but modified values of OAS content according to two approaches:

(1) "Vertical" approach, in which the upwelling and downwelling of the layer with maximum OAS content is simulated. Figure 2 shows an example for upwelling analysis, where the vertical profile of chl-a concentration is varied in 1 m increments and the corresponding *Rrs* spectrum is calculated. This approach will also be applicable for internal wave analysis.

(2) "Horizontal" approach, where the vertical profiles of OAS content inside the hydrodynamic structure, layer by layer, are replaced by interpolated "background" values of vertical profiles outside the hydrodynamic structure. Figure 3 is an example for analyzing the Z_{rs} depth for a submesoscale eddy, where Fig. 3a presents a simulation of the removal of the eddy structure from the upper layers to the lower layers.

The deepest layer that is obtained in a vertical or horizontal approach, in which the hydrodynamic structure will have $|\text{CNR}| > 1$ for at least one of the remotely determined characteristics, will be the detection depth of hydrodynamic structure Z_{rs}.

It should be borne in mind that to determine the type of hydrodynamic structure it is not enough that $|\text{CNR}|$ exceeds the threshold value. It is important to have some number of pixels (measurement points), in the area of the assumed process, by which the corresponding structures will be identified. For example, from a single point, even with a large $|\text{CNR}|$, it is not always possible to say that a hydrodynamic structure is observed. Conversely, if there are many nearby pixels, but with small values $|\text{CNR}| \approx 1$ or even $0.5 < |\text{CNR}| < 1$ in the area of hydrodynamic processes, such a structure can be identified by modern pattern recognition methods. From this point of view, it is important that Z_{rs} is a "maximum" depth, i.e., it can be perceived as an estimate of the value "from above". Even if in reality at the obtained depth value Z_{rs} the number of measurement points with sufficient $|\text{CNR}|$ will be insufficient to identify the hydrodynamic structure, it means that at the depth (Z_{rs} – 1 m) they will become much more, since the process of manifestation of hydrodynamic structures in the spectral data on sea color is not linear in depth.

CONCLUSIONS

A method has been developed that makes it possible to determine the thickness of the water surface layer, where the upwelling radiation is formed with the possibility of identifying the hydrodynamic structure in the water color remote sensing data. This method allows to improve the interpretation of remotely sensed data of the water upwelling radiation associated with the vertical variability of the content of optically active substances in the aquatic environment and hydrodynamic processes

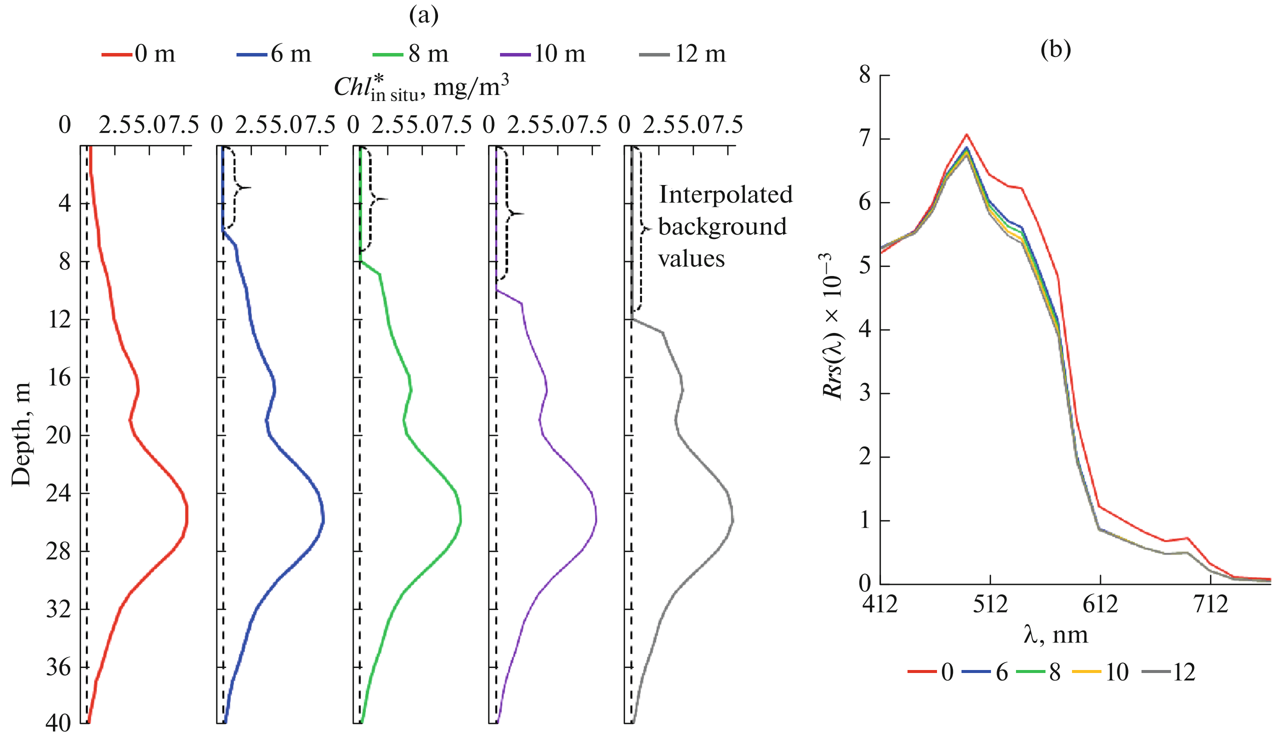

Fig. 3. (a) Example of simulation of the change in eddy structure due to a change in the vertical profile of the chl-a (Chl_{insitu}) concentration leading to a decrease in contrast in remotely sensed data; (b) results of direct numerical simulation of *Rrs* as a function of the thickness of the upper sea layer in which the eddy structure is removed.

[9, 10, 17], and can be used in laboratory and numerical experiments, as well as in field studies. Also, the results obtained can be used for laser sensing of the water column [18, 19], and as an extension for complex optical, microwave and acoustic systems for remote sensing of the water column [20–22].

FUNDING

The presented study is performed within the state tasks of the Il'ichev Pacific Oceanological Institute, Far Eastern Branch, Russian Academy of Sciences, and projects no. 124022100080-0, 124042300003-5.

CONFLICT OF INTEREST

The authors of this work declare that they have no conflicts of interest.

REFERENCES

1. Choi, J.K., Park, Y.J., Ahn, J.H., Lim, H.S., Eom, J., and Ryu, J.H., *J. Geophys. Res: Oceans*, 2012, vol. 117, no. C9, p. C09004. https://doi.org/10.1029/2012JC008046
2. Kubryakov, A.A., Lishaev, P.N., Chepyzhenko, A.I., Aleskerova, A.A., Kubryakova, E.A., Medvedeva, A.V., and Stanichny, S.V., *Oceanology*, 2021, vol. 61, p. 159. https://doi.org/10.1134/S0001437021020107
3. Salyuk, P.A., Mosharov, S.A., Frey, D.I., Kasyan, V.V., Ponomarev, V.I., Kalinina, O.Yu., Morozov, E.G., Latushkin, A.A., Sapozhnikov, Ph.V., Ostroumova, S.A., Lipinskaya, N.A., Budyansky, M.V., Chukmasov, P.V., Krechik, V.A., Uleysky, M.Yu., Faiman, P.A., Mayor, A.Yu., Mosharova, I.V., Chernetsky, A.D., Shkorba, S.P., and Shved, N.A., *Water*, 2022, vol. 14, no. 23, p. 3879. https://doi.org/10.3390/w14233879
4. Mobley, C.D., *Light and Water: Radiative Transfer in Natural Waters*, San Diego: Academic, 1994.
5. Gordon H. R. Brown, O.B., Evans, R.H., Brown, J.W., Smith, R.C., Baker, K.S., and Clark, D.K., *J. Geophys. Res.: Atmos.*, 1988, vol. 93, no. D9, p. 10909. https://doi.org/10.1029/JD093iD09p10909
6. Zaneveld, J.R.V., Barnard, A.H., and Boss, E., *Theor. Opt. Express*, 2005, vol. 13, p. 9052. https://doi.org/10.1364/OPEX.13.009052
7. Hedley, J.D. and Mobley, C.D., *HYDROLIGHT 6.0 ECOLIGHT 6.0 Technical Documentation*, Tiverton: Numerical Optics, 2019.
8. Mobley, C.D., Chai, F., Xiu, P., andSundman, L.K., *J. Geophys. Res.*, 2015, vol. 120, p. 875. https://doi.org/10.1002/2014JC010588
9. Salyuk, P.A., Glukhovets, D.I., Lipinskaya, N.A., Moiseeva, N.A., Churilova, T.Ya., Ponomarev, V.I., Aglova, E.A., Artemiev, V.A., Latushkin, A.A., and Major, A.Yu., *Sovrem. Probl. Distantsionnogo Zondirovaniya Zemli Kosm.*, 2021, vol. 18, no. 6, p. 200. https://doi.org/10.21046/2070-7401-2021-18-6-200-213

10. Lipinskaya, N.A., Salyuk, P.A., and Golik, I.A., *Remote Sens.*, 2023, vol. 15, no. 23, p. 5600. https://doi.org/10.3390/rs15235600
11. Mueller, J.L., *Ocean Optics Protocols for Satellite Ocean Color Sensor Validation*, Revision 4: *Introduction, Background, and Conventions*, Goddard Space Flight Center, 2003, vol. 1.
12. Hu, C., Lee, Z., and Franz, B., *J. Geophys. Res.: Oceans*, 2012, vol. 117, no. C1, p. C01011. https://doi.org/10.1029/2011JC007395
13. Tonizzo, A., Twardowski, M., McLean, S., Voss, K., Lewis, M., and Trees, C., *Appl. Opt.*, 2017, vol. 56, p. 130. https://doi.org/10.1364/AO.56.000130
14. Welvaert, M. and Rosseel, Y., *PLoS One*, 2013, vol. 8, p. e77089. https://doi.org/10.1371/journal.pone.0077089
15. Matkovic, K., Neumann, L., Neumann, A., Psik, T., and Purgathofer, W., *Comput. Aesthet. Graph.*, 2005, vol. 9, p. 159. https://doi.org/10.2312/COMPAESTH/COMPAESTH05/159-167
16. O'Reilly, J.E. Maritorena, S., Mitchell, B.G., Siegel, D.A., Carder, K.L., Garver, S.A., Kahru, M., and McClain, C., *J. Geophys. Res.: Oceans*, 1998, vol. 103, no. C11, p. 24937. https://doi.org/10.1029/98JC02160
17. Nosov, V.N., Kaledin, S.B., Ivanov, S.G., and Timonin, V.I., *Opt. Spectrosc.*, 2019, vol. 127, p. 669. https://doi.org/10.21883/OS.2019.10.48366.165-19
18. Pershin, S.M., Brysev, A.P., Grishin, M.Y., Lednev V.N., Bunkin A.F., and Klopotov R.V., *Bull. Russ. Acad. Sci.: Phys.*, 2021, vol. 85, p. 665. https://doi.org/10.3103/S1062873821060174
19. Bukin, O.A., Pavlov, A.N., Saluk, P.A., Golik, S.S., Ilin, A.A., and Bubnovskii, A.Yu., *Opt. Atmos. Okeana*, 2010, vol. 23, no. 10, p. 926.
20. Peshekhonov, V.G., Mashoshin, A.I., Shafranyuk, A.V., Korchak, V.Yu., Kovalenko, V.V., Luchinin, A.G., Malekhanov, A.I., Mareev, E.A., Smirnov, I.P., Khil'ko, A.I., Kravchenko, V.N., and Prikhod'ko, I.M., *Bull. Russ. Acad. Sci.: Phys.*, 2016, vol. 80, p. 1229. https://doi.org/10.3103/S1062873816100130
21. Makarov, D.V., Uleysky, M.Yu., and Prants, S.V., *Tech. Phys. Lett.*, 2003, vol. 29, no. 5, p. 430. https://doi.org/10.1134/1.1579816
22. Ermakov, S.A., Kapustin, I.A., and Sergievskaya, I.A., *Bull. Russ. Acad. Sci.: Phys.*, 2010, vol. 74, p. 1695. https://doi.org/10.3103/S1062873810120166